

## BUBBLE DYNAMICS UNDER AN IMPINGING PLANAR WATER JET

Ahmed, A. B. and Hamed, M. S.\*

\*corresponding Author

Thermal Processing Laboratory (TPL), Department of Mechanical Engineering,

McMaster University,

Hamilton, ON, Canada

E-mail: hamedm@mcmaster.ca

### ABSTRACT

The limiting factor in many industries is the maximum operating temperature and/or the maximum heat flux to be dissipated from the surface. Liquid Jet Impinging Cooling (LJIC) is one of the most effective cooling means because of its high heat transfer coefficient. LJIC is extensively used in steel quenching, electronic chips cooling and emergency rapid core cooling in nuclear reactors. Though, the surface heat flux has no straight forward formula. The present study adapts the mechanistic modeling approach to quantify the surface heat flux under different conditions. The mechanistic model assumes that the heat is transferred from the surface through multiple mechanisms, namely: boiling, forced convection and transient conduction. The total wall heat flux is calculated as the algebraic sum of these different heat flux components. The boiling heat transfer component depends on bubbles behaviour on the surface (bubble dynamics). Bubble growth rate, departure diameter, release frequency and number of bubbles on the surface are the major bubble dynamics parameters that are affected by the jet. This paper presents the result of an experimental investigation of bubble dynamics under a planar water jet. The experimental data are collected using high speed imaging of the boiling process at different degrees of superheating. Results reported here are for a 0.85 m/s jet. The jet was found to suppress nucleation close to the impinging zone and deform growing bubble from the spherical shaper. Away from stagnation, bubble diameter was found to depend on the square root of growth time, i.e.  $D \sim \sqrt{t_g}$

### INTRODUCTION

The capability of LJIC of carrying away high heat from the surface is due to the thin thermal boundary layer on the surface and the boiling liquid. The heat transfer coefficient is as high as 10 kW/m<sup>2</sup> and even higher in the mode of boiling. The capability of the LJIC in removing high heat transfer rates from the surface is due to the thin thermal boundary layer on the surface and the boiling liquid [1].

The fluid under the jet can be divided into three main zones, as shown in Figure 1: stagnation zone, acceleration zone and parallel flow zone. At the stagnation zone, the impinging jet raises the pressure to its maximum value with a zero parallel velocity component. As the flow changes to become parallel to the surface, the pressure decreases and the stream wise velocity increases till both the pressure and velocity reaches their steady value in the parallel flow zone [1].

### NOMENCLATURE

$C_p$	[J/kg.K]	Specific heat
$D$	[m]	Bubble diameter
$E$	[J]	Energy
$F$	[N]	Force
$Fr$	[-]	Froude number $V_1 / \sqrt{gH}$
$h_{fg}$	[J/kg]	Latent heat of vaporization
$k$	[W/mK]	Thermal conductivity
$q$	[W/m <sup>2</sup> ]	Heat flux
$t$	[S]	Time
$T$	[K]	Temperature
$V$	[m/s]	Velocity
$x$	[m]	Distance from the jet centre
$Y$	[m]	Free surface height
$\Delta T$	[K]	Temperature difference (T-T <sub>sat</sub> )

#### Special characters

$\rho$	[kg/m <sup>3</sup> ]	Density
$\theta$	[°]	Camera angle

#### Subscripts

$b$	Buoyancy
$cp$	Contact pressure
$du$	Asymmetrical bubble growth
$fc$	Forced Convection
$g$	Growth
$h$	Hydrodynamic
$qs$	Quasi-steady drag
$sl$	Shear lift
$sub$	Subcool
$sup$	Superheat
$tc$	Transient conduction
$w$	Wall or waiting

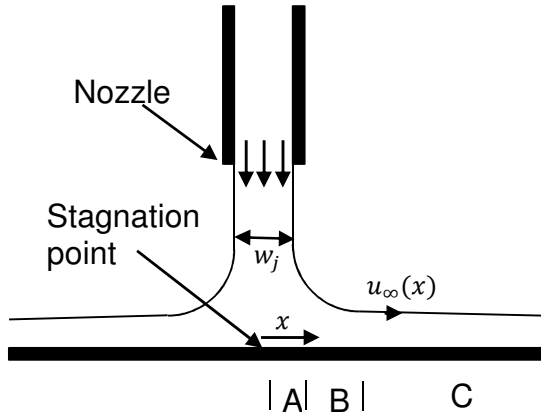


Figure 1 Free-planar jet A: Stagnation Zone B: Acceleration Zone C: Parallel flow Zone [1]

Several studies [1-5] have been carried out to estimate the wall heat flux of boiling heat transfer under a subcooled liquid jet. The main aim of these studies was to model the wall heat flux in terms of the known flow and surface conditions. These models can be classified into two main types based on the way the wall heat flux is modeled:

- Global models
- Mechanistic models.

A brief discussion about each modeling technique is provided below with a quick review of the most significant research related to what presented in this work.

### GLOBAL MODELING OF THE WALL HEAT FLUX

Global modeling is relatively easy and fast technique to estimate wall heat flux. It uses empirical correlations to predict the wall heat flux without much focus on the contribution of the different heat transfer mechanisms. Moreover, the models are limited to the experimental data used to develop and validate, which limits their generality. The heat flux in fully developed boiling under an impingement subcooled jet can be correlated as,

$$q_w = C \Delta T_{sup}^n \quad (1)$$

where  $C$  and  $n$  are constants determined empirically. Hall et al. [2] determined  $C$  and  $n$  for the stagnation region. Although their experiments showed dependency on jet velocity, other researchers reported no noticeable change in the heat flux with jet velocity [1]. Also, other researchers [3], [4] indicated that before the Onset of Nucleate Boiling (ONB), the heat flux increases with the jet velocity and there is no significant effect of the jet velocity after ONB.

Ishigai et al. [5] carried out transient and steady state jet boiling experiments and found that the boiling curve is shifted up and to the right with the increase of jet velocity at high degrees of subcooling.

Although global modeling technique allows to estimate the wall heat flux and the constants are relatively easy to be obtained, it doesn't provide details about the physical mechanisms of heat transfer associated the boiling phenomena under impinging jets.

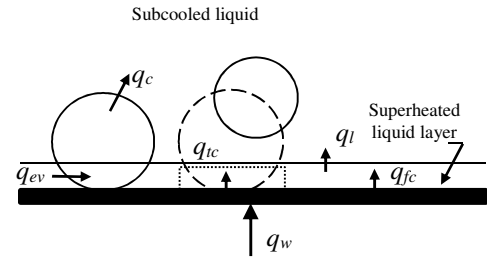
### MECHANISTIC MODELING OF THE WALL HEAT FLUX

Mechanistic modeling is used as an attempt to overcome global modeling limitations and to have a better understanding of the physics of the boiling process; the boiling surface is partitioned to regions which one or many governing heat transfer mode is/are prevalent. Before the ONB, the wall heat flux is assumed to be equal to the heat transferred by forced convection only and is expressed as,

$$q_w = q_{fc} = h_{fc} (\Delta T_{sup} + \Delta T_{sub}) \quad (2)$$

Unlike flow boiling, the heat transfer coefficient in the case of jet impinging boiling varies over the heated surface due to jet hydrodynamics and the inviscid flow effects. The boundary layer development from the impinging zone till the parallel flow zone also has an effect on the temperature and heat flux on the surface [1].

At the ONB, the single phase convection is enhanced due to the turbulence caused by the existence of the bubbles on the surface. It is assumed that bubbles are not attached to the surface statically. Rather, bubbles start growing and departing the surface once ONB is reached. The bubble departures, either lifts off or slides on the surface, disturbs the subcooled liquid layer allowing the subcooled liquid to come in contact with the surface initiating transient conduction heat transfer, as shown in Figure 2. The transient conduction is assumed to be one-dimensional conduction into a semi-finite liquid kept at  $T_l$  exposed to a constant temperature surface at  $T_w$ . It worth noting that all the heat from the wall is assumed to be transferred to the superheated layer first. The heat transfer from this layer is assumed to be the



main cause of the liquid evaporation and the bubble growth.

Figure 2 Representation of the heat transfer paths to the liquid

The wall heat flux can be expressed as,

$$q_w = q_{fc} + q_{ic} \quad (3)$$

where the enhanced heat transfer coefficient,  $h_{fc}$ , is directly affected by the nucleation site density. The transient conduction will prevail till the time  $t_{ic}$  at which the transient conduction is equal to the single phase heat flux, transient conduction can be expressed as,

$$q_{ic} = \frac{1}{t_w + t_g} \int_0^{t_{ic}} \frac{k_l}{\sqrt{\pi \alpha_l t}} (\Delta T_{sup} + \Delta T_{sub}) dt \quad (4)$$

$$t_{ic} = \frac{\rho_l C_p K_l}{\pi h_{fg}^2} \quad (5)$$

## CLOSURE SUBMODELS

As each component of the partitioned wall heat flux is evaluated independently and explicitly, a group of submodels is required to find closure of the wall heat flux and each component. These submodels depend on experimental observations to find the effect of the global parameters i.e., with the jet velocity, degree of subcooling and superheat. The applicability of these models is confined by the area on the surface over which each heat transfer mechanism occurs.

## BUBBLE GROWTH SUBMODEL

One of the most important submodels is the bubble growth submodel. Bubble growth rate and its lift off diameter from the surface is of interest. Previous work [6] indicated that the balance between the forces acting on the bubble results in bubble departure from nucleation site, while balance between heat transfer from the surface and to the bulk liquid is the reason for bubble growth or decay. There is scarcity in the literature of bubble dynamics model under impinging liquid jets. The only existing model is the one developed by Omar et al. [6] which did not consider all forces acting on the bubble, such as the surface tension force. In his model, Omar addressed four forces acting on the bubble during its growth, namely: the drag force, the instantaneous force because of the flow; the growth force, as the fluid is displacing the surrounding liquid; the buoyancy force, caused by the density difference; and the shear lift force, acting in the normal direction.

As the bubble grows, the magnitude of forces components acting onto it changes. The bubble leaves the surface when the drag and buoyancy forces overcome the surface tension force. In other words, bubble lift off happens when  $\sum F_y = 0$  condition is no longer valid, while bubble sliding along the heater surface happens when  $\sum F_x = 0$  is not valid anymore. The area over which different heat transfer mechanisms occur is affected by how the bubble departs its nucleation site, whether the bubble will slide or lift off.

There are three possibilities for the bubble, as shown in Figure 3, it will grow till it (1) lifts off from the surface or (2) collapses locally or (3) slides along the surface and then it lifts off or collapses. Omar [6] developed a procedure to determine if the bubble would slide (scenario I) or collapse locally on the surface (scenario II). He only considers the two cases of bubble thermal growth and then collapse or bubble sliding; his models do not consider bubble lift off the surface which is the case in most of the bubbles on the surface after ONB. Experimental observations confirmed that the bubble slides on the surface after it leaves its nucleation site and then lifts off. Many researchers investigated forces balance of bubble in case of pool boiling and flow boiling [7–11]. In this work, we readdress the force balance on the bubbles in order to develop a more comprehensive model of all bubble termination scenarios. In the current model, the forces considered are: the drag force, the buoyancy force, the expansion (liquid inertia) force, and the shear lift force, and the surface tension force [12]. Order of magnitude analysis has been carried out to determine the significance of each force.

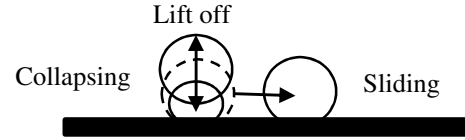


Figure 3 Schematic of bubble departure: sliding or lift off

The force balance in both parallel and normal to the flow can be written as,

$$\sum F_x = F_{\sigma,x} + F_{qs} + F_{du,x} \quad (6)$$

$$\sum F_y = F_{\sigma,y} + F_{du,y} + F_{sl} + F_h + F_{cp} + F_b \quad (7)$$

Where surface tension,  $F_{\sigma,x}$ , quasi-steady drag force,  $F_{qs}$ , asymmetrical bubble growth,  $F_{du,x}$ , act in the x-direction. In the y direction, surface tension,  $F_{\sigma,y}$  asymmetrical bubble growth,  $F_{du,y}$ , shear lift force,  $F_{sl}$ , hydrodynamic,  $F_h$ , contact pressure,  $F_{cp}$ , and buoyancy,  $F_b$ , are the acting forces.

## EXPERIMENTAL SETUP

### A. TEST SECTION

A 10 mm wide, 30 mm long, and 6 mm thick copper block surface is exposed to a planar water jet. The copper block is heated by three 25  $\mu\text{m}$ -thick NiCr 80/20 foils. A thin layer of thermally conductive-electrically insulating material is pressed between the foils and the copper block to eliminate any electrical contact with low contact thermal resistance. The three foils are heated as a DC current from three power supplies pass through them. Their output currents are controlled separately to achieve uniform surface temperature. This approach comes as the one heater design failed attaining uniform surface temperature; the foil was long enough that different heat transfer modes are present at time on the surface. For example, one end of the heater is the stagnation zone while the other end has nucleate boiling on the surface.

The water is pumped from a thermostat controlled water tank. The loop is fitted with the necessary measuring devices to know the flow conditions: water flow rate, water temperature, line pressure.

The surface is prepared for before each experiment. It is pressed against a fine sandpaper for 1 minute then cleaned with acetone. The surface roughness was measured, at two different points on the surface on the surface after two random preparation procedure and it was around 110 nm.

### B. TEMPERATURE MEASUREMENT AND CONTROL

Two rows of nine-0.5mm K-type thermocouples are inserted half way through holes in the copper block. The holes were filled with thermal oil and holes top are sealed with high temperature silicone. K-type thermocouples are used because they are known

for their minimal thermal drift over long period of time and at high temperatures. The three foils are connected to the three power suppliers which are controlled independently through LabVIEW software package. The objective is to maintain the uniform surface temperature regardless of the surface heat flux mechanism. Although attaining constant surface temperature is one of the biggest challenges in heat transfer and boiling studies, a number of trails were conducted to find the optimum control scheme. First, proportional controller was adapted to reach the system the steady state conditions. For steady state offset problem in proportional controller, Proportional Integral (PI) controller is used. PID controllers are not recommended for such an application as the noise in temperature measurement would cause an instability issues [13]. The two coefficients of the PI controller are set and tested experimentally to ensure steady state operation and to avoid overheat of the NiCr foil which cause the burnout of the foil.

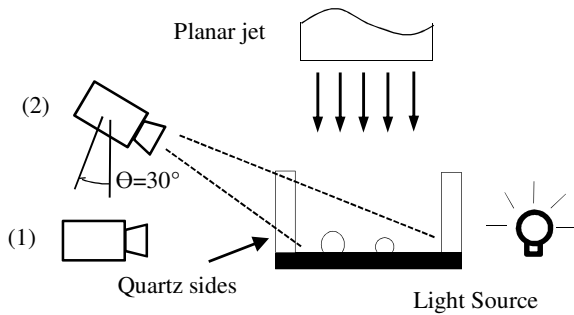


Figure 4 Experimental section layout

### C. HIGH SPEED IMAGING

Starting the ONB, bubbles are present on the surface. Bubbles intensity and frequency increase with wall superheat till fully developed nucleate boiling and the bubble covers the whole surface. The ebullition process is pictured with high frames per rate pictures, up to 6000 fps, at different surface temperatures from ONB till fully developed boiling. The camera was set at first parallel to the surface, position (1) in Figure 4, giving real dimensions and fast processing of the bubbles. Yet, the distribution of the bubbles on the surface was not controlled and the bubbles close to the camera will hide other bubbles (in the middle) behind it. Tilting the camera was considered, position (2) in Figure 4. Although tilting the camera at the surface requires correcting the measured lengths and angles measured, it widens the frame and allow more bubbles to be pictured. By setting a scale onto the surface, vertical dimensions measured could be corrected as follows,

$$L_{actual} = L_m / \cos \theta \quad (8)$$

Where  $\theta$  is camera tilt angle and  $l_m$  is the measured length.

### HYDRAULIC JUMP

A change in the flow height happens downstream of the jet when a supercritical flow ( $Fr > 1$ ) is turned into a subcritical flow ( $Fr < 1$ ) by a flow obstruction. It's usually accompanied with loss in energy because of the turbulence in the transition region.

$$E_{loss} = E_1 - E_2 = (y_1 + V_1^2 / 2g) - (y_2 + V_2^2 / 2g) \quad (9)$$

For Froude numbers from the critical value,  $Fr=1$ , to  $Fr=1.7$ , the transition is very smooth and hardly noticeable. The higher the Froude number, the more rollers intensity. For Froude numbers between 4.5 and 9 the rollers are completely contained and does not affect the surface smoothness which is the case for this work [14].

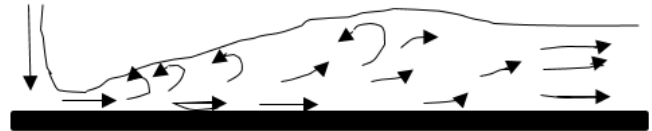


Figure 5 Hydraulic jump for Fr 4.5 to 9 [14].

### RESULTS AND DISCUSSION

The surface of the copper was pictured under water jet velocity of 0.85 m/s and 7 °C of subcooling. The taken pictures gives insightful information about bubble departure diameter, growth rate and progression of first bubble on the surface.

The following results and discussion are based on analysis of the pictures using image processing software. Taking pictures with 6000 fps, the camera was able to capture bubble growth as shown in Figure 7. Diameter of the bubble was measured every two frames with an uncertainty of  $\pm 0.12$  mm

Bubble growth is fast in the beginning and then the bubble grows slower as the bubble volume increases. As the Thermal Boundary Layer (TBL) is thinner in case of impingement jet than flow boiling or pool boiling, the bubble diameter is bigger than the TBL causing condensation at the top of the bubble; condensation is balanced with evaporation happens in the TBL. That might be the reason why bubble size doesn't increase rapidly or collapse as it is close to lift off from the surface. Bubble continues to grow to the point at which the vertical forces on it act to detach it from the surface. If this moment delayed as the vertical forces are not enough to detach the bubble, it sometimes experience more condensation resulting in lowering bubble diameter. Bubble growth is proportional to the square root of growth time within TBL as shown in Figure 7. The proportionality constant was found to be 1.4. For the same degree of superheat, lift off diameter is found to be linearly proportional to the time the bubble takes to detach from the surface as shown in Figure 8.

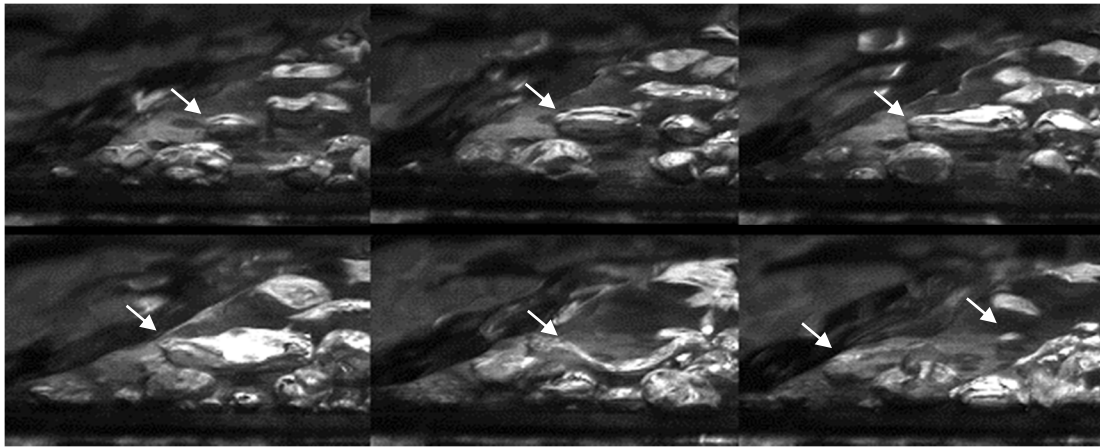


Figure 6 Bubble growing under the impinging jet

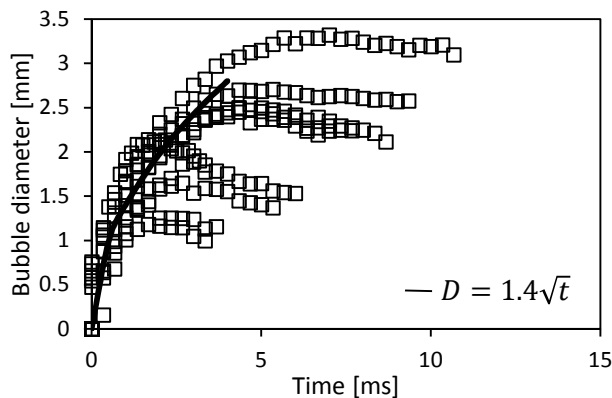


Figure 7 Different bubble growth diameter with growth time for one nucleation site 15 mm away from the jet at  $\Delta T_{sup}=10^{\circ}\text{C}$ ,  $\Delta T_{sub}=7^{\circ}\text{C}$

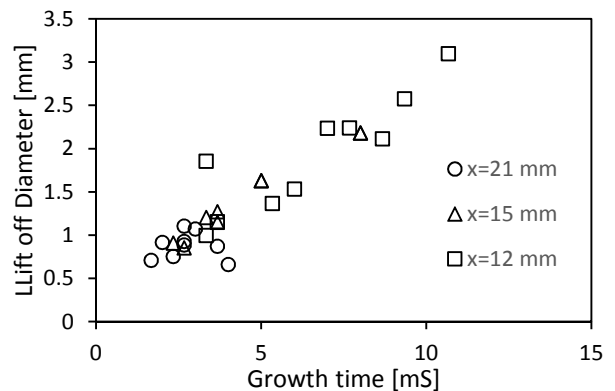


Figure 8 Bubble lift off diameter vs bubble lift off time  $\Delta T_{sup}=10^{\circ}\text{C}$   $V_j=0.85$  m/s

Each nucleation site was found to release bubbles within a specific range of diameters. For example, the most probable bubble diameters lie between 0.9 mm to 3.3 mm for nucleation site 15 mm away from the jet as shown in Figure 7. Also, for the same nucleation site, the lift off diameter was traced over many frames for different degrees of superheat. For example at 12 mm away from the jet, the lift off diameter is found to increase with the degree of superheat. It increased from 0.9 mm at degree of superheat of  $10^{\circ}\text{C}$  to 2 mm at  $15^{\circ}\text{C}$ .

The effect of the jet dynamics is clear as the bubble lift off diameter tend to increase the further its location from the jet. As all the pictured bubbles are after the hydraulic jump start, bubbles closer to the jet are subject to higher velocities. The jet effect is also clear in the closest active nucleation site to the jet. Bubbles in impinging region the bubble loses its spherical shape and start to flatten under the velocity of the jet. The bubble grows in spherical shape until it reaches certain diameter after which the bubble continues to grow laterally more than vertically and usually split into two bubbles. This can be seen in Figure 6 as well as bubble split into two bubbles because of the jet.

Bubbles in the transition length from supercritical to subcritical flow are smaller in diameters than bubbles grow away from the jump. Rollers and swirls over the jump length cause either earlier lift off or suppress the bubbles. The further from the jet impinging region, the lower ONB degree of superheat as shown in Figure 9. This is because of two reasons: (1) the rollers and swirls in the flow and (2) the growth of the TBL over the parallel flow region.

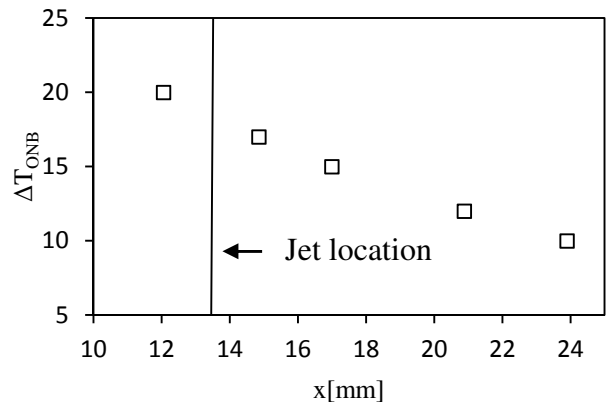


Figure 9 Location of the first bubble on the surface

## CONCLUSION

An experimental study of bubbles dynamics under a planar water jet has been carried out. Results indicate the effect of jet hydrodynamics in suppressing the bubbles under the jet (impinging zone) till higher degree of superheat ( $22^{\circ}\text{C}$ ) at which the heat flux out of the surface is enough to grow a bubble. Bubbles growing under the jet are severely affected by the jet which flattens it and even split it into two bubbles in some cases. Away from the stagnation zone, bubbles were observed in the hydraulic jump and was found to be affected by the flow field after the jump. Bubble diameter during growth is found to be proportional to the square root of the growth time while the lift off diameter is linearly proportional to the lift off time.

## REFERENCES

- [1] Wolf D., and Incropera F., Jet impingement boiling, *Advances in heat transfer*, vol. 23, 1993, pp. 1–132
- [2] Hall D., Incropera F., and Viskanta R., Jet impingement boiling from a circular free-surface jet during quenching: part I—single-phase jet, *Journal of Heat Transfer*, vol. 123, no. 5, 2001, pp. 901–910
- [3] Wang X. and Monde M., Critical heat flux in forced convective subcooled boiling with a plane wall jet (Effect of Subcooling on CHF), *Heat and Mass Transfer*, vol. 33, no. 1–2, Sep. 1997, pp. 167–175
- [4] Zhou D. and Ma C., Local jet impingement boiling heat transfer with R113, *Heat and Mass Transfer*, vol. 40, no. 6–7, Aug. 2003, pp. 539–549
- [5] Ishigai S., Nakanishi S., and Ochi T., Boiling heat transfer for a plane water jet impinging on a hot surface, *Sixth International Heat Transfer Conference*, 1987, pp. 445–4450
- [6] Omar A., Hamed M., and Shoukri M., On the bubble dynamics under an impinging free planar jet, *ECI International Conference of Boiling Heat Transfer*, 2009, pp. 421–428
- [7] Siedel S., Cioulachtjian S., Di Bari S., Robinson A., and Bonjour J., Experimental investigation on the local curvature of bubble interface during boiling on a single nucleation site, *ECI 8th International Conference on Boiling and Condensation Heat Transfer*, June 2012, pp. 3–7
- [8] Zuber N., Hydrodynamic aspects of boiling heat transfer, *Los Angeles and Ramo-Wooldridge Corporation*, 1959.
- [9] Van Helden W., Forces on bubbles growing and detaching in flow along a vertical wall, *International Journal of Heat and Mass Transfer*, vol. 38, no. 94, 1995.
- [10] Zeng L., Klausner J., and Mei R., A unified model for the prediction of bubble detachment diameters in boiling systems—I. Pool boiling, *International Journal of Heat and Mass Transfer*, vol. 36, no. 9, Jan. 1993, pp. 2261–2270
- [11] Zeng L., Klausner J., Bernhard M., and Mei R., A unified model for the prediction of bubble detachment diameters in boiling systems—II. Flow boiling, *International Journal of Heat and Mass Transfer*, vol. 36, no. 9, Jan. 1993, pp. 2271–2279
- [12] Klausner J., Mei R., Bernhard D., and Zeng L., Vapor bubble departure in forced convection boiling, *International Journal of Heat and Mass Transfer*, vol. 36, no. 3, 1993, pp. 651–662
- [13] Blum J. and Marquardt W., Stability of boiling systems, *International Journal of Heat and Mass Transfer*, vol. 39, no. 14, 1996, pp. 3201–3033
- [14] Chow V., Open-Channel Hydraulics, *McGraw-Hill*, New York, NY, 1959.